ACS OMEGA

http://pubs.acs.org/journal/acsodf

Article

# Hydrocortisone-Loaded Lipid−Polymer Hybrid Nanoparticles for Controlled Topical Delivery: Formulation Design Optimization and In Vitro and In Vivo Appraisal

Omar Awad Alsaidan, Mohammed Elmowafy,* Khaled Shalaby, Sami I. Alzarea, Diaa Massoud, Abdulsalam M. Kassem, and Mohamed F. Ibrahim

Cite This: *ACS Omega* 2023, 8, 18714−18725

Read Online

ACCESS | Metrics & More | Article Recommendations | Supporting Information

**ABSTRACT:** The barrier functionalities of the skin offer a major but not insuperable hindrance for fabrication of skin delivery effective systems. This work aimed to develop an optimized lipid polymer hybrid nanoparticle and assess the skin delivery effectiveness of hydrocortisone ($9.872 \pm 0.361 \times 10^{-3}$ $cm^2/h$) of a drug through the skin from an optimized formulation when compared with a drug solution. Meanwhile, histological examination after topical application of the optimized formulation showed a safe increase in epidermal thickness. In vivo, the optimized formulation showed promising anti-inflammatory activity in a croton oil-induced ear rosacea model. As an excellent anti-inflammatory agent, these findings propose that the use of lipomers could be a promising strategy to improve the topical effectiveness of hydrocortisone acetate (HCA) against inflammatory diseases. Collectively, these results support our view that lipid polymer hybrid nanoparticles can proficiently deliver hydrocortisone to the skin in treating skin inflammatory conditions.

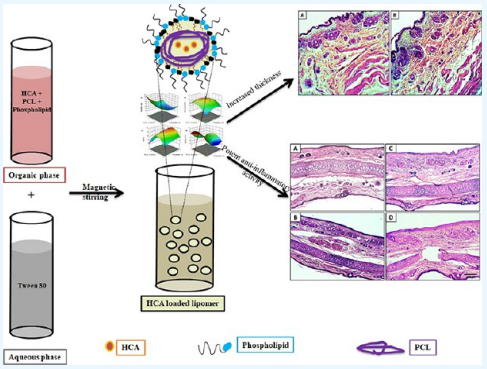


## 1. INTRODUCTION

Skin disorders are considered as one of the most common diseases influencing about 30 to 70% of the population, producing a heavy burden in the worldwide context of public health.[1] The occurrence and accompanying cost of these illnesses surpass those of other illnesses, including diabetes and cardiovascular diseases.[2] Among them, chronic inflammatory skin disorders are arbitrated by multifaceted immunological aspects. Atopic dermatitis is one of chronic and relapsing inflammatory skin disorders manifested by intense itching, disruption of the skin barrier, cutaneous dryness, and inflammatory eczema.[3] This skin disorder requires a thorough skin care and therapeutically effective treatment since it has a massive influence on patient quality of life. Of the different accessible treatment approaches for this disease, local corticosteroids have powerful anti-inflammatory efficacy. They are efficient at monitoring quickly worsening atopic dermatitis and are considered among the main acclaimed strategies to treat the disease.[4] Nonetheless, adverse effects after long-term topical application of corticosteroids, including skin atrophy, hypopigmentation, and secondary infection, have confined their use, particularly the potent ones.[5]

Hydrocortisone is a category V−VII, low-to-intermediate-potency corticosteroid with excellent anti-inflammatory and vasoconstrictive effects.[6] It was the first drug of the synthetic corticosteroid category that was utilized in local skin formulations for this indication. However, addition of the acetate group to its structure was reported to enhance the local activity fivefold. On the other hand, hydrocortisone acetate was reported to induce both local and systemic adverse effects, including skin atrophy, erythema, skin dryness, and suppression of the hypothalamus−pituitary−adrenal gland axis.[7] In addition, skin permeability of hydrocortisone acetate (HCA) was reported to be low when using raw materials.[8]

Nanocarriers are considered one of the most proficient systems used for skin delivery.[9] Polymer−lipid hybrid nanoparticles are viewed as a potential system for drug delivery. It is composed of a polymeric core and a phospholipid shell. Thus, it gathers the advantages of both liposomes and polymer nanoparticles.[10,11] According to the type of polymer, it can encapsulate hydrophobic or hydrophilic drugs as well as control drug release. On the other hand, the phospholipid shell surrounds the core and offers the biocompatibility of the system as well as minimizes drug escape from the polymeric core.[12] Preparation of polymer−lipid hybrid nanoparticles requires at least three chief constituents, i.e., the lipid, the polymer, and the

Received: January 31, 2023
Accepted: May 10, 2023
Published: May 19, 2023

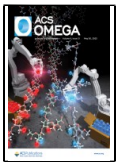

active molecule. Nevertheless, selection of the constituents and their concentrations is important in fabricating formulation possessing acceptable performance. Thus, we selected polycaprolactone (PCL) as a hydrophobic polymer to encapsulate the hydrophobic drug, hydrocortisone. To obtain adequate delivery of hydrocortisone through the skin after topical application, we selected the concentration of phospholipid, a skin penetration-enhancing agent, as one of independent variables during optimization design. However, we selected polymer−lipid hybrid nanoparticles to deliver HCA to skin as it can control drug release (due to polymeric content), which confines transdermal absorption, which is a desirable action to minimize frequent administration and subsequent local and systemic side effects.

Taking all this into consideration, the current work was designed to fabricate and optimize the hydrocortisone-loaded polymer−lipid hybrid nanoparticles by using the combination of phospholipid and polymer through the Design-Expert tool. PCL was selected as the polymer for the entrapment of hydrocortisone as it is a biocompatible and biodegradable lipophilic polymer and can encapsulate hydrophobic drugs efficiently and the phospholipid (Phospholipon 90 G) for covering the polymeric core, which simulates the skin lipids and helps the penetration of the fabricated system. Design-Expert was utilized to optimize a set of formulations with a two-factor, three-level design. The responses included particle size, zeta potential, encapsulation efficiency, and release in a sustainable pattern in order to obtain an optimized formulation. In addition, the optimized formulation was tested for morphology, drug crystallinity, stability, ex vivo skin permeation, and in vivo pharmacodynamic efficacy.

## 2. MATERIALS AND METHODS

**2.1. Materials.** HCA, PCL (Mw: 70,000−90,000 Da) and Tween 80 were purchased from Sigma-Aldrich. Phospholipid (Phospholipon 90 G; PC) was kindly obtained from Lipoid (Switzerland). Acetone (purity >99%) and ethanol (95%) were obtained from Sigma-Aldrich (Germany). All other chemicals and solvents were of analytical grade.

**2.2. Fabrication of HCA-Loaded Lipomers.** HCA-loaded lipomers were prepared by a single-step nanoprecipitation method.[13] The organic phase was prepared by separately dissolving PCL in acetone (with gentle heating) and phospholipid and HCA in ethanol. Then, the solutions were mixed together with continuous stirring. The aqueous phase was prepared by dissolving Tween 80 (surfactant) into bi-distilled water. The organic phase was then carefully dropped into the aqueous phase (ratio 3:1, respectively) with incessant magnetic stirring, and the resultant dispersion was kept overnight. After that, the dispersion was centrifuged at 12,000 rpm for 0.5 h to separate lipomer pellets, which were re-suspended in the bi-distilled water by vortexing (Dragonlab cortex, China) to achieve uniform dispersion.

**2.3. Experimental Design.** Lipomers were designed and optimized by Design-Expert software with a two-factor, three-level Box−Behnken statistical design. Eleven formulations were produced including eight factorial and three center points. Two factors, nominated phospholipid concentration A (1−10) and the concentration of Tween 80-B (0.5−3%), were expected to influence the production of lipomer formulations (Table 1). The responses are the particle size ($Y_1$), zeta potential ($Y_2$), entrapment efficiency % (EE%) ($Y_3$), and HCA release ($Y_4$). The desired outcomes were to decrease the particle size, increase both zeta potential ($Y_2$) and EE% ($Y_3$), and control HCA release. The compositions of the all batches are illustrated in Table 2.

**Table 1. Levels of Independent Variables and Dependent Variables Used in Experimental Design**

| | | levels | | |
|---|---|---|---|---|
| | | low | medium | high |
| factor | process parameter | (−1) | (0) | (1) |
| | **Independent variables** | | | |
| A | **phospholipid concentration (mg/mL)** | 1 | 5 | 10 |
| B | **concentration of Tween 80** | 0.5% | 1.5% | 3% |
| **Responses** | | **Desired outcome** | | |
| $Y_1$ | particle diameter | decreased | | |
| $Y_2$ | zeta potential | increased | | |
| $Y_3$ | encapsulation efficiency % | increased | | |
| $Y_4$ | HCA release | controlled | | |

**Table 2. Compositions and Responses According to Box−Behnken Design**

| std | run | phospholipid conc. | surfactant conc. | PS (nm) | ZP (mV) | EE% | % release |
|---|---|---|---|---|---|---|---|
| 9 | 1 | 5.5 | 1.75 | 236.5 | −21.5 | 87.9 | 73.9 |
| 3 | 2 | 1 | 3 | 348.9 | −26.9 | 71.2 | 85.9 |
| 7 | 3 | 5.5 | 1.125 | 229.8 | −23.6 | 83.9 | 69.5 |
| 1 | 4 | 1 | 0.5 | 321.5 | −34.2 | 75.5 | 76.5 |
| 10 | 5 | 5.5 | 1.75 | 237.6 | −22 | 88.1 | 74.3 |
| 8 | 6 | 5.5 | 2.375 | 284.3 | −28.6 | 84.6 | 70.9 |
| 4 | 7 | 10 | 3 | 275.9 | −27.6 | 76.3 | 65.9 |
| 6 | 8 | 7.75 | 1.75 | 259 | −26.9 | 89.6 | 72.9 |
| 2 | 9 | 10 | 0.5 | 268.3 | −30.9 | 78.9 | 58.9 |
| 5 | 10 | 3.25 | 1.75 | 254.8 | −24.6 | 83.8 | 81.6 |
| 11 | 11 | 5.5 | 1.75 | 239.8 | −20.9 | 87.6 | 74 |

**2.4. Particle Size and Zeta Potential.** The dynamic light scattering approach was used to determine the particle size and zeta potential using the Zetasizer analyzer (Malvern, UK) at a temperature of 25 °C. Batches were appropriately diluted with bi-distilled water, vortexed, and measured thrice.

**2.5. EE%.** EE% of lipomer batches was determined by the direct method reported by Gajra et al.[14] Formulations were centrifuged at 12,000 rpm for 0.5 h, supernatants were removed, and the sediments were dissolved in a dichloromethane/ethanol mixture (1:1, v/v). The HCA concentration was determined using a UV−visible spectrophotometer (Genesis, China) at 248 nm[15] after construction of the linear concentration versus absorbance calibration curve. EE% was calculated using eq 1:

$$\text{EE\%} = \frac{\text{amount of HCA in pellets}}{\text{tota amount of HCA added}} \times 100 \quad (1)$$

**2.6. In Vitro HCA Release.** The in vitro release of HCA from different batches was done using a Franz-diffusion cell device connected with an autosampler (Logan DHC-6 T Dry Heating Transdermal System). Aliquot samples of HCA-loaded lipomers (1 mL equivalent to 5 mg of HCA) were placed onto cellulose membranes (molecular weight cutoff: 12,000−14,000 Da) tightly sealed to one side of the glass set and considered as comprising a donor compartment. The acceptor compartment consisted of 12 mL of PBS/ethyl alcohol (70/30, v/v; pH = 5.5) to maintain skin conditions, and the temperature was kept at 37 ± 0.5 °C. Aliquots of the acceptor compartment (1 mL) were removed at different time intervals up to 12 h to quantify HCA


https://doi.org/10.1021/acsomega.3c00638
ACS Omega 2023, 8, 18714−18725

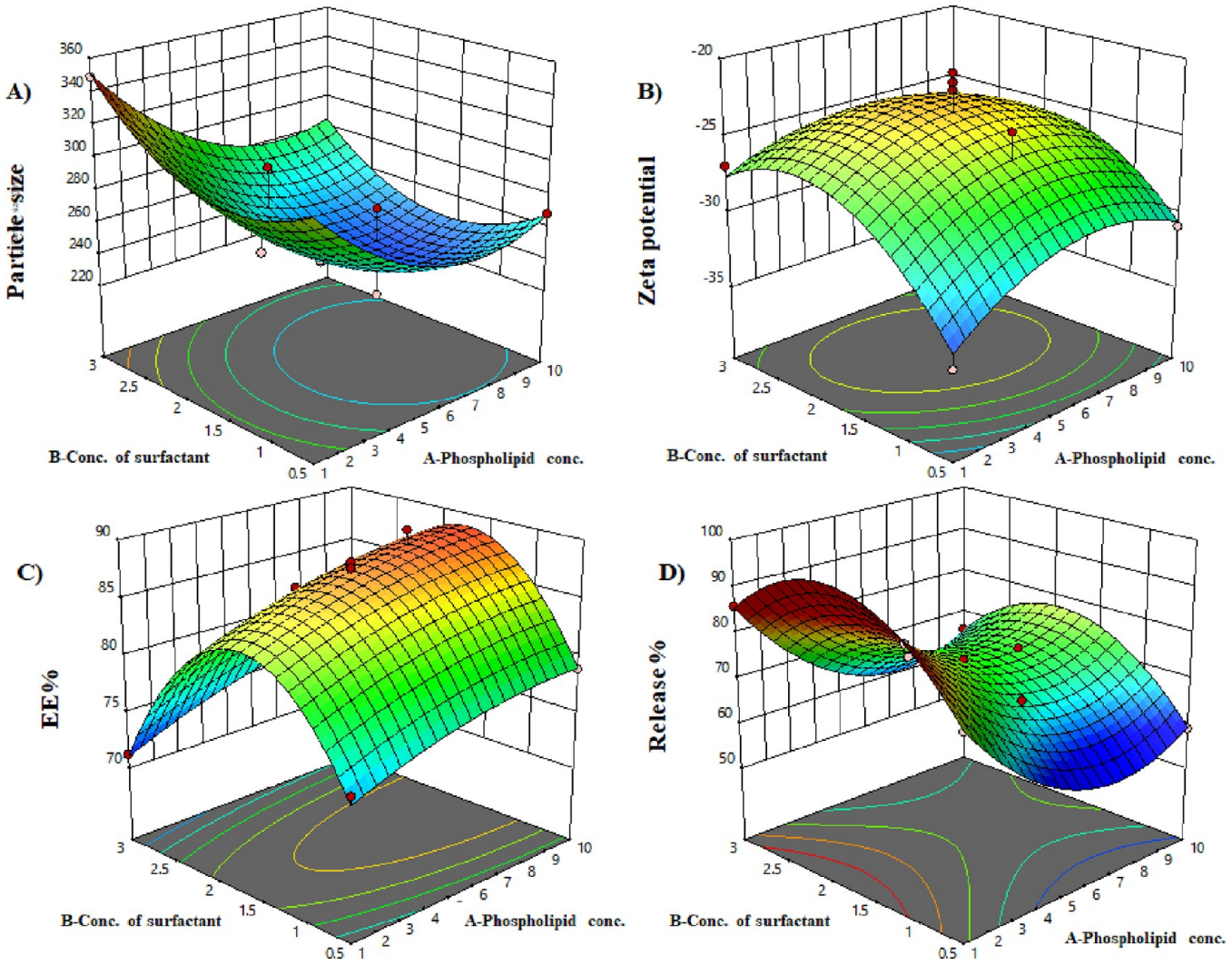


**Figure 1.** 3D surface response for the influence of different independent variables on (A) particle size, (B) zeta potential, (C) EE%, and (D) drug release.

spectrophotometrically, and the acceptor compartment was replenished with an equal volume of fresh medium to keep a constant volume. The percentage of HCA release was plotted versus time to study the release behavior of the studied formulations.

**2.7. Morphology.** The optimized formulation was characterized for surface topography using transmission electron microscopy (TEM; JEOL, Japan). The sample was diluted by double-distilled water and dropped on a carbon grid. The grid was allowed to air dry and then imaged.

**2.8. Thermal Analysis Using Differential Scanning Calorimetry (DSC).** DSC (DSC3, Mettler Toledo, Switzerland) is a technique used to check the interaction between compositions of the formulation referring to the transition temperature of the raw materials and after formulating the batch under investigation. The thermal analyses of HCA, PCL, phospholipid, and lyophilized optimized formulation were carried out. Five milligrams of each sample was put in an aluminum pan and placed in the appropriate place in a device cell. The empty pan was used as a reference. The heating scan rate was 10 °C/min, and the temperature was recorded between 25 and 280 °C. Peaks were automatically identified using STAR$^e$ 15.00 software.

**2.9. Fourier Transform Infrared Spectroscopy (FTIR).** FTIR is another tool used to investigate the drug/excipient interaction through identification of the function groups in both raw materials and formulation. FTIR (FTIR; Thermo Scientific) analyses were performed for HCA, PCL, phospholipid, and lyophilized optimized formulation. The scan was done in the range between 4000 and 400 $cm^{-1}$ in transmission mode.

**2.10. Short-Term Stability Study.** A stability study of the optimized formulation was carried out by measurements of particle size, zeta potential, and EE% after 1 month of storage at ambient (25 ± 1 °C) and refrigerator (4 ± 0.5 °C) temperatures in stoppered glass containers.

**2.11. Ex Vivo Skin Permeation Study.** Ex vivo skin permeability was carried out on hairless full-thickness rabbit skin using Franz diffusion cells by the same conditions mentioned above in section In Vitro HCA Release. The studies performed on animals were conducted according to the ethical procedures and policies of Jouf University (Bioethical Code: 8/01/43). Skin was mounted to the cells where the stratum corneum was directed to the upper direction and faced the formulation under investigation. Endoderm was directed to the acceptor compartment (12 mL of PBS/ethyl alcohol (70/30, v/v; pH = 5.5)). An aliquot of 1 mL of the optimized formulation or HCA solution


https://doi.org/10.1021/acsomega.3c00638
ACS Omega 2023, 8, 18714−18725

was put onto the stratum corneum. Samples (0.5 mL) from the acceptor compartment were withdrawn at different time points, and HCA was quantified spectrophotometrically. An equal volume of fresh medium was added to the acceptor compartment to keep a constant volume. All measurements were carried out in triplicate. Data was then fitted to different kinetic models (zero-order kinetics, first-order kinetics, Higuchi diffusion model, and Korsmeyer−Peppas model) to study the appropriate permeation mechanism based on the value of correlation coefficient ($R^2$).

After obtaining the permeation data, the percentage of permeated HCA was plotted against time points. Then, permeation parameters were calculated as follows: flux (*Jss*, $\mu g/cm^2/h$) via the skin from the optimized formulation and HAC solution was determined by dividing the slope of the straight part of the graph by an area of diffusion (1.14 $cm^2$), the apparent permeability coefficient (*Kapp*, cm/h) was calculated by multiplying the receptor compartment volume by the original HCA concentration ($C_0$) in the donor compartment by flux,[16] and the enhancement ratio (ER) was calculated by dividing the flux of the optimized formulation by the flux of the HCA solution.

**2.12. Post-Application Histological Changes.** In comparison with untreated animals, cutaneous alterations after application of the optimized formulation were evaluated by topical application once daily for three successive days. Concisely, the dorsal side hairs were removed and the animals were allocated into two groups (five rabbits for each group). Group 1 was kept as the untreated control group whereas group 2 was treated with topical application of the optimized formulation. At the end of the experiment, areas of application (2 $mm^2$ tissue margin) of the rabbits that were sacrificed were cut and instantaneously dipped in Serra fixative for about 48 h. Tissue samples were dehydrated in ascending series of ethyl alcohol, cleared in xylol, and embedded in paraffin wax. Then, the samples were adapted vertically in plastic paraffin blocks. For histological investigations, sectioning with 7 $\mu$m was conducted using a rotary microtome (Leica RM2125 RTS, USA) and mounted on clean and dry glass slides. The slide sections were deparaffinized in xylol, hydrated again in descending series of ethyl alcohol till the water was distilled, immersed in hematoxylin for about 15 min, washed in tap water, and kept in eosin for 45 s. Finally, the stained sections were dehydrated and cleared again, mounted in DPX, covered with cleaned glass slides, and left to dry at 55 °C overnight. The stained sections were examined and photographed using a Boeco light microscope supplied with a digital camera. For statistical analysis to assess the permeation of the optimized formulation, the epidermal thickness of 20 measurements was recorded for the control and treated groups using ImageJ software. The obtained data were expressed in means ± SD. The results were considered statistically significant if the probability is less than 0.05.

**2.13. Anti-Inflammatory Effect.** In order to assess the anti-inflammatory effect of the optimized formulation, a croton oil model was used to induce rabbit ear inflammation.[17] Rabbits were divided into four groups (five animals for each rabbit). Group 1 was kept as the untreated control group whereas group 2 (toxic group) was treated with local application of 10 $\mu$L of croton oil solution (prepared in 3% solution in acetone). Groups 3 and 4 were treated with local application of the HCA solution and the optimized formulation, respectively, after 15 min from application of croton oil. Rabbit ears were cut after ether inhalation, and the procedure mentioned in Section 2.9 was followed to evaluate the pharmacodynamic efficacy.

**2.14. Statistical Analysis.** The results are displayed as means ± standard deviations (SD). The statistical analysis was performed using one-way analysis of variance (ANOVA), and means were compared using Tukey's multiple-comparison testing. Probability ($P$) less than 0.05 was considered to be significant.

## 3. RESULTS AND DISCUSSION

**3.1. Rationale and Formulations of HCA-Loaded Lipomers.** Among the various skin delivery systems, lipomers were selected as a promising system to deliver HCA to the skin. Undeniably, lipomers have been chosen by several investigators to enhance the oral delivery of drugs suffering from poor oral bioavailability.[14,18−20] However, in literature, the system has been utilized for skin delivery to a lesser extent.[21,22] Combining lipid and polymer in a single nanocarrier offers a distinctive system to provide both efficient skin-penetrative power (phospholipid can fuse to skin lipids and then diffuse drug molecules across skin layers) and a controlled release pattern (PCL offers a sustained release behavior), which are needed in treatment of local chronic diseases such as atopic dermatitis and

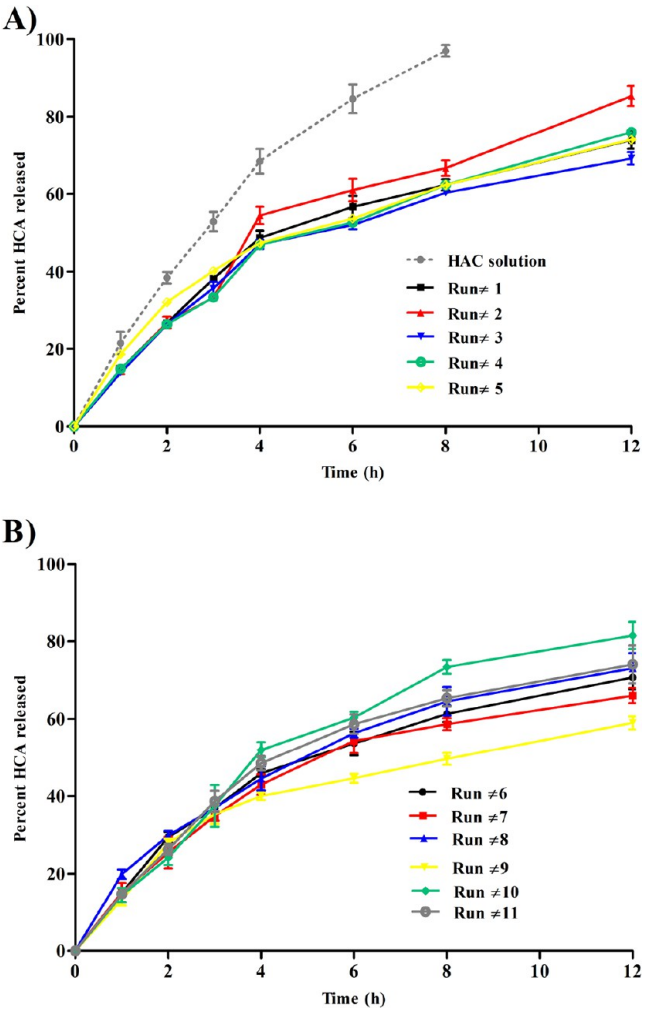


**Figure 2.** In vitro release profiles of HCA from different batches: (A) HCA solution and runs 1−5, and (B) runs 6−11 (mean values ± SD, $n$ = 3).


https://doi.org/10.1021/acsomega.3c00638
ACS Omega 2023, 8, 18714−18725

**Table 3. Actual and Predicted Values of Independent Variables and Responses for the Optimized Formulation**

| | independent variables | | dependent variables | | | | |
|---|---|---|---|---|---|---|---|
| formula | level of factor A | level of factor B | particle size (nm) | zeta potential (mV) | EE% | release% | desirability |
| predicted | 8.2 | 0.675 | 251.45 | −28.2 | 81.5 | 58.91 | 0.972 |
| actual | 8.2 | 0.675 | 249.7 | −27.3 | 82.7 | 61.7% | |

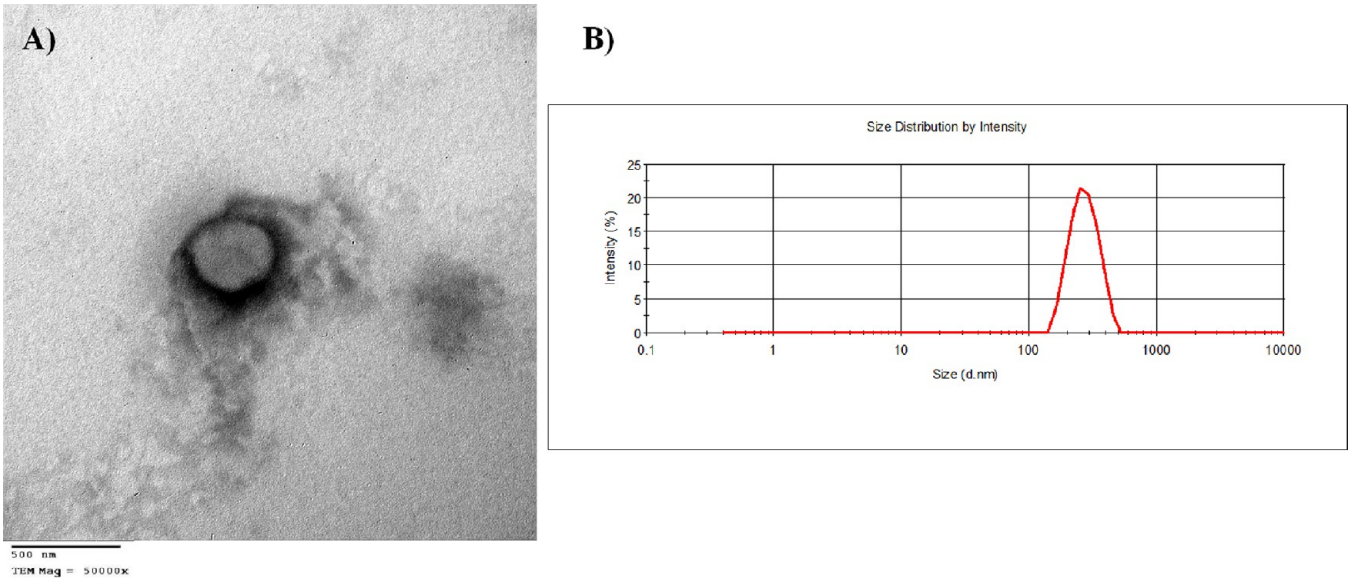


**Figure 3.** (A) TEM image and (B) size distribution graph of the optimized formulation.

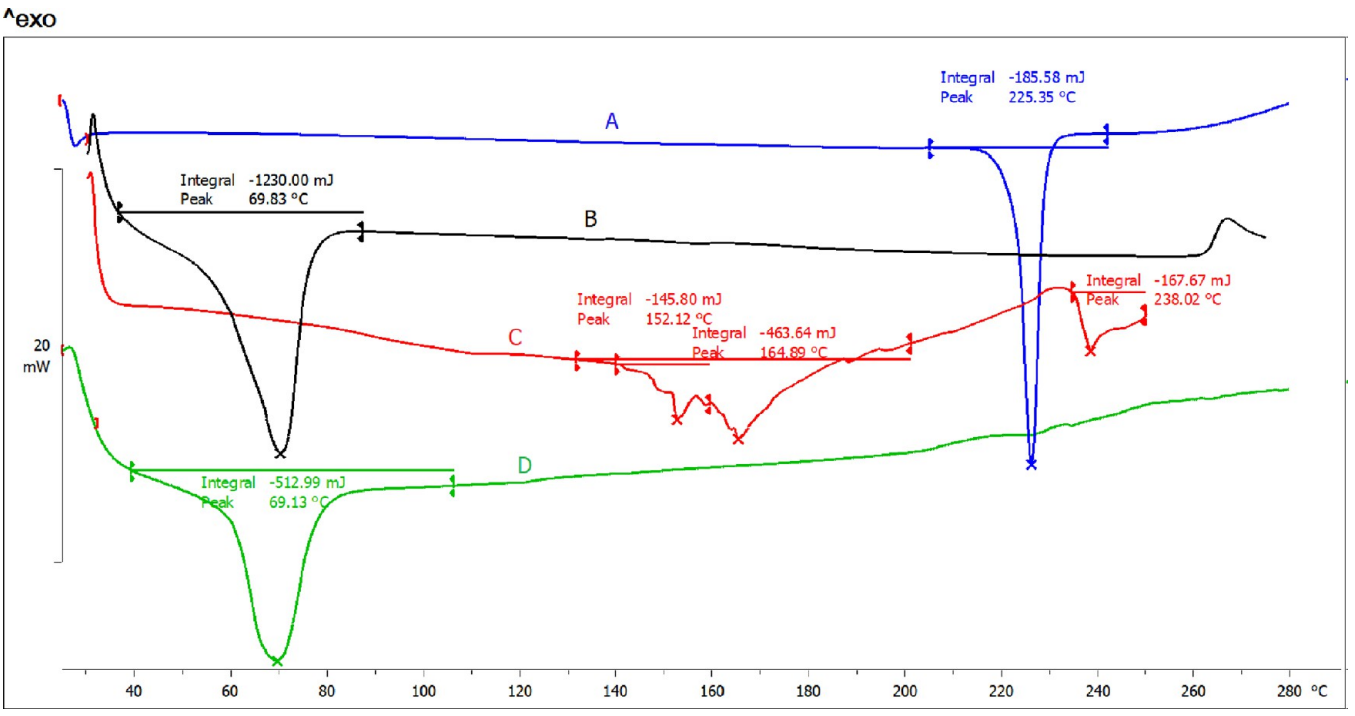


**Figure 4.** DSC thermograms of (A) HCA, (B) PCL (C) phospholipid, and (D) optimized formulation.

chronic inflammatory skin diseases. We studied the influence of phospholipid concentration and the concentration of the surfactant on particle size, zeta potential, EE%, and release.

**3.2. Box−Behnken Design Analysis and Optimization.** A two-factor, three-level Box−Behnken design was utilized to investigate quadratic response surfaces with Design-Expert software including 11 experimental runs. The independent variables selected were A-phospholipid concentration and B-concentration of the surfactant, while particle size ($Y_1$), zeta potential ($Y_2$), EE% ($Y_3$), and HCA release ($Y_4$) were the selected dependent responses. The findings of the 11 investigated batches are outlined in Table 2. 3D plots are outlined for all the four responses in Figure 1. The non-linear quadratic model was found to be the best model of fit to



https://doi.org/10.1021/acsomega.3c00638
ACS Omega 2023, 8, 18714−18725

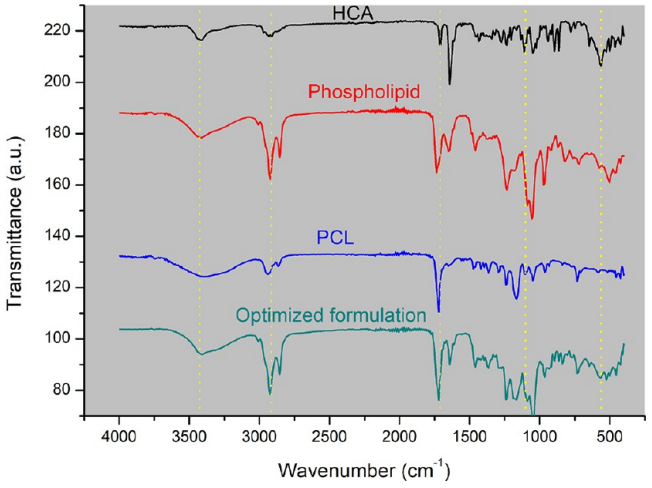


**Figure 5.** FTIR spectra of HCA, phospholipid, PCL, and the optimized formulation.

**Table 4. Stability Studies of the Optimized Formula in Ambient and Refrigerating Temperatures within 1 Month (Mean ± SD; $N = 3$)**

| assessment criteria | storage conditions | freshly prepared | after 1 month |
|---|---|---|---|
| particle size (nm) | at 25 ± 1 °C | 249.7 ± 16.8 | 263.2 ± 13.6 |
| | at 4 ± 0.5 °C | 249.7 ± 16.8 | 265.7 ± 18.1 |
| zeta potential (mV) | at 25 ± 1 °C | −27.3 ± 2.5 | −25.3 ± 7.5 |
| | at 4 ± 0.5 °C | −27.3 ± 2.5 | −26.9 ± 5.8 |
| EE% | at 25 ± 1 °C | 85.7 ± 4.6 | 82.4 ± 14.8 |
| | at 4 ± 0.5 °C | 85.7 ± 4.6 | 84.1 ± 9.5 |

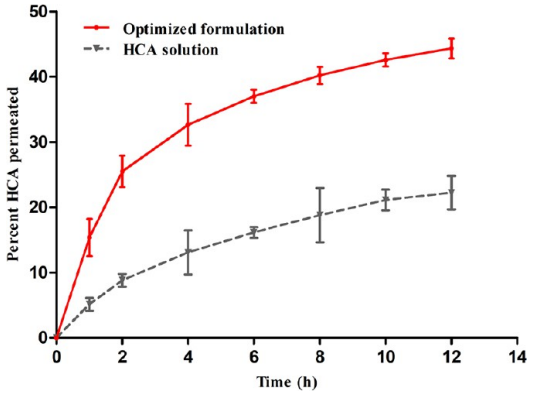


**Figure 6.** Representative graph of the percentage cumulative amounts of HCA permeated through full-thickness skin samples versus time for the optimized formulation and the HCA solution (mean values ± SD, $n = 3$).

interpret the effect of independent variables (A-polymer/lipid ratio, and B-concentration) on the responses (Table S1 in the Supporting Information).

*3.2.1. The Influence of Independent Variables on Particle Size.* For skin delivery, the diameter of the particle in the system is a key element. In general, the smaller the particle's diameter, the higher the cutaneous adhesion and occlusion exhibited by the system. It is obvious that the particle size of the 11 runs varied between 229 and 348.9 nm (Table 2), and the results depended on the level of independent variables and interactions between them. Run 2 showed the largest particle diameter (348.9 nm), while run 3 showed the smallest particle diameter (229 nm). Figure 1A shows the influence of the independent variables and their interactions on the particle size.

The polynomial equation of particle size is outlined below (eq 2):

$$Y_1 = +244.15 - 27.58A + 13.83B - 4.95AB + 29.78A^2 + 30.38B^2 \quad (2)$$

The equation indicates that the phospholipid concentration significantly ($P < 0.05$) influenced the diameter of lipomers. As factor $A$ was negatively signed, it had an inverse relation with the particle size, i.e., the higher the phospholipid concentration, the smaller the particle size. In fact, all batches were designed at a fixed concentration of the polymer (PCL; 10 mg/mL). Hence, increasing the phospholipid concentration could indirectly decrease the polymeric concentration in the total loaded nano-matrix. Conversely, using a low-concentration phospholipid could indirectly increase the polymeric concentration in the total nano-matrix. This increment in the particle diameter at greater polymeric concentrations could be attributed to production of highly viscous dispersion.[23] This highly viscous dispersion could influence the particle diameters either by reducing the evaporation rate of the organic solvent[24] or by creating more resistant dispersion to the breakdown of the particles via reducing the influence of shear force generated by the stirring[25] and resisting the particles' collision.[26] On the other hand, the phospholipid is a well-established surface active agent. Therefore, using a high concentration might contribute to reducing the interfacial tension and hence the particle size.[14]

It is clear from Figure 1A that the particle diameters were initially decreased upon increasing the concentration of the surfactant until reaching the center point (1.75%), after which the particle size began to increase again. At initial low concentrations, the surfactant molecules were not adequate to cover the particles of lipomers. By a gradual increase, the molecules of surfactants could efficiently cover the particles' surfaces leading to a reduction in the interfacial tension between the solvent phases.[14] By a further increase in surfactant concentration, surfactant aggregates could form[27] and/or fuse to and adhere onto the lipomer particles, leading to an increase in the diameters of the particles.[28]

*3.2.2. The Influence of Independent Variables on Zeta Potential.* The zeta potential of the colloidal system is a key element in stability determination. Usually, the higher the absolute zeta potential value than 20, the greater the stability of the system due to greater repulsive forces between particles.[29] As illustrated in Table 2, the values of the zeta potential of the developed formulations ranged from −34.2 mV (run 4) to −20.9 mV (run 11). Generally, the negative value of the surface charge is formed due to the presence of the negative phosphate

**Table 5. Ex Vivo Skin Permeation Parameters for the Optimized Formulation and the HCA Solution**

| formulation | flux, *Jss* ($\mu g/cm^2/h$) | apparent permeability coefficient *Kapp* × $10^2$ (cm/h) | Q/A ($\mu g/cm^2$) | enhancement ratio (ER) |
|---|---|---|---|---|
| optimized form | 0.987 ± 0.141 | 11.84 ± 1.29 | 38.88 ± 5.1 | 1.5 |
| HCA solution | 0.663 ± 0.162 | 7.95 ± 1.4 | 19.50 ± 2.8 | |



https://doi.org/10.1021/acsomega.3c00638
ACS Omega 2023, 8, 18714−18725

**Table 6. Fitting of Ex Vivo Skin Permeation Data of Optimized Formulation with Different Kinetic Models**

| | zero-order kinetics | | | first-order kinetics | | | Higuchi model | | | Korsmeyer–Peppas model | | |
|---|---|---|---|---|---|---|---|---|---|---|---|---|
| formulation | $R^2$ | $K_0$ | $t_{1/2}$ | $R^2$ | $K_1$ | $t_{1/2}$ | $R^2$ | $K_H$ | $t_{1/2}$ | $R^2$ | $n$ | $t_{1/2}$ |
| optimized formulation | 0.509 | 4.65 | 10.74 | 0.698 | 0.065 | 10.69 | 0.950 | 14.17 | 12.44 | 0.987 | 0.361 | 15.19 |

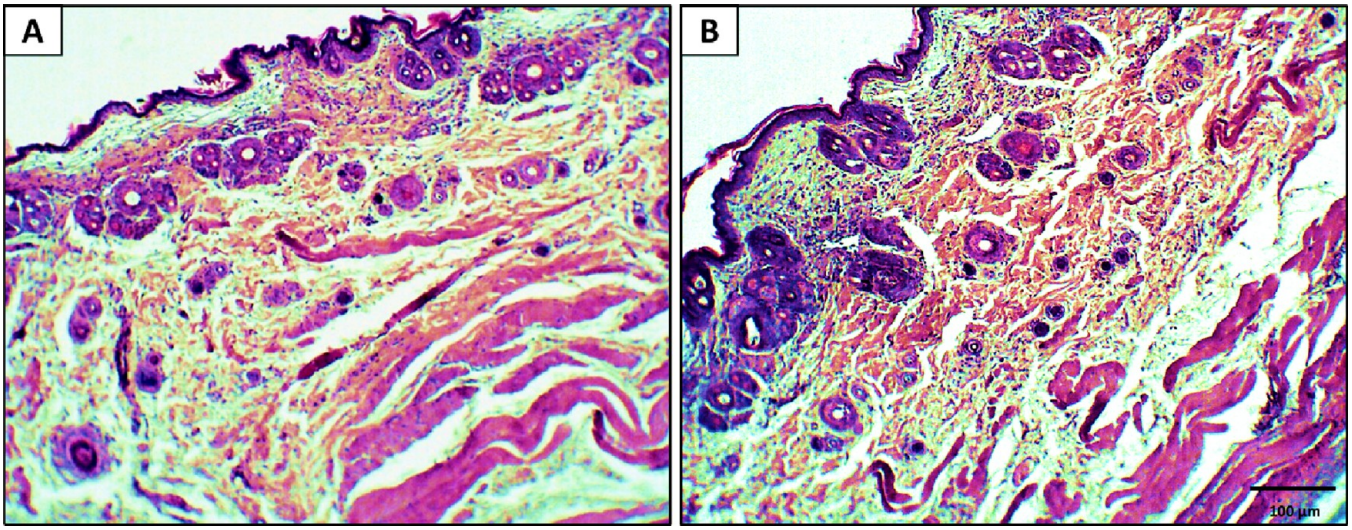


**Figure 7.** Photomicrographs of rabbit dorsal skin sections of the (A) control and (B) optimized formulation-treated groups stained with hematoxylin and eosin at a magnification of 100×, scale bar = 100 $\mu$m for all groups.

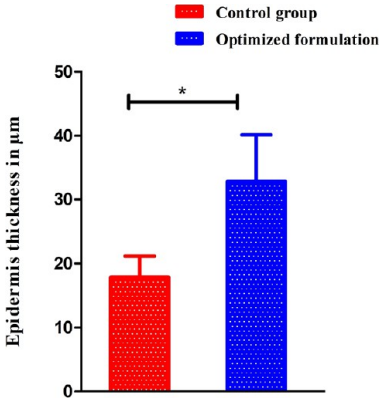


**Figure 8.** Epidermal thickness of the skin of the control group (untreated group) and after topical application of the optimized formulation.

group in phospholipid.[30] This indicates that the system was composed of lipid shell around the polymeric core.

Figure 1B shows the 3D response surface plot for the zeta potential representing the influence of the studied factors. The polynomial equation of the zeta potential is outlined below (eq 3):

$$Y_2 = -23.42 + 0.322\mathrm{A} + 1.8B - 1.0AB - 2.65A^2 - 4.05B^2 \quad (3)$$

From the equation above, the concentration of phospholipid did not substantially influence the surface charge of lipomer batches. On the other hand, the concentration of the surfactant (Tween 80) influenced the zeta potential value. Run 4 (containing the lowest concentration of the surfactant) presented the highest negativity among all investigated formulations. Tween 80, as a non-ionic surfactant, was reported to oppose the negativity of the anionic nature of phospholipid, leading to a decrease in the negativity of the formulations upon increasing the surfactant concentration.[31]

*3.2.3. The Influence of Independent Variables on EE%.* EE% represents the amount of the drug encapsulated in the formulation, which is an essential factor for assessment of colloidal systems. EE% of the 11 runs ranged between 71.2 and 89.6% (Table 2), depending on the level of each factor and the interaction between them. Run 8 exhibited the highest EE%, while run 2 showed the lowest EE% among all investigated formulations. Figure 1C shows the 3D response surface plot for the EE% showing the effect of independent variables.

The polynomial equation of EE% is outlined below (eq 4):

$$Y_3 = +87.38 + 2.53A - 1.46B + 0.425AB - 1.08A^2 - 10.88B^2 \quad (4)$$

The equation explains the influence of different factors on the EE% of lipomer formulations. In Figure 1C, it is observed that by increasing the concentration of phospholipid, there was increase in the EE%. This behavior might be attributed to an increase in the thickness of the lipid layer,[32] upon using a higher concentration of phospholipid, leading to incorporation of some drug molecules into the lipid layer and a decrease in the escaping of the drug into the external phase.[14]

The concentration of the surfactant had a substantial effect on the EE% of the developed batches. Upon increasing the amount of the surfactant, an initial increase in EE% was observed until reaching the central point, followed by a decline in EE%. It is suggested that the surfactant was effectively adsorbed on the surface of phospholipid (verified by partial neutralizing of the negative value of the zeta potential), leading to modification of the surface properties and reduction in the Gibbs free energy.[33] After the central point, the increase in surfactant concentration had a negative effect on EE%. This behavior might be attributed to an increase in the partitioning of the drug molecules into the aqueous external phase due to higher solubility of the drug in it


https://doi.org/10.1021/acsomega.3c00638
ACS Omega 2023, 8, 18714−18725

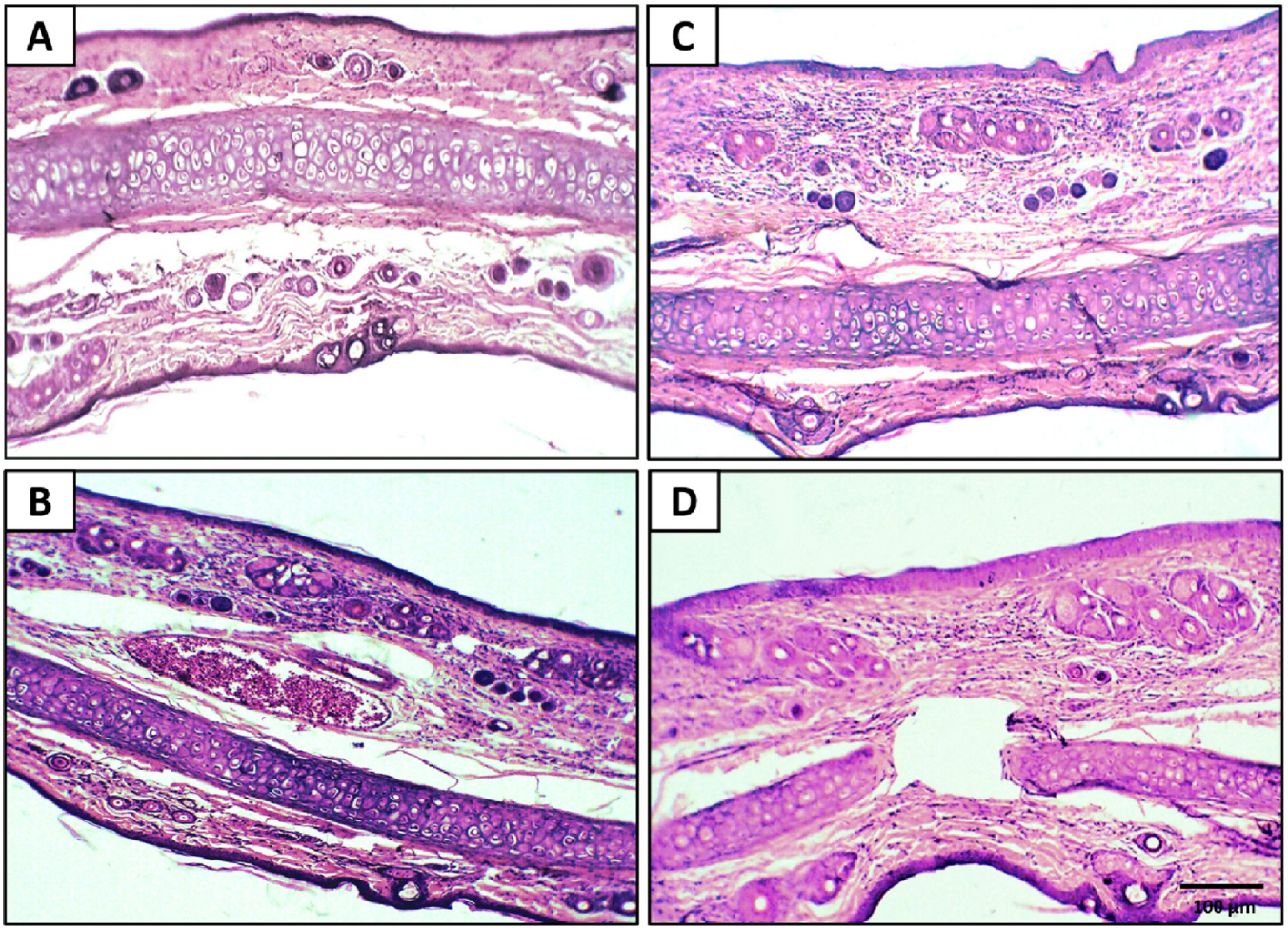


**Figure 9.** Photomicrographs of the rabbit ear sections of the (A) control untreated group, (B) toxic group, (C) HCA solution-treated group, and (D) optimized formulation-treated group stained with hematoxylin and eosin at a magnification of 100×, scale bar = 100 $\mu$m, for all sections. (C) The HCA solution-treated group displays relatively mild infiltration of neutrophils when compared to the toxic group. HCA can efficiently act as an anti-inflammatory drug through different mechanisms including immunosuppressive effect, which inhibits immunoglobulin G antibody and suppresses both T-cell proliferation and dendritic cell maturation. It also prevents leukocyte migration to the skin inflammation areas.[55,56] In addition, HCA acts as a vasoconstrictor within the upper layers of the skin, which indirectly decreases the inflammation by minimizing the blood flow to the inflammation site.[6] Application of the optimized formulation (Figure 9D) induced a higher healing effect when compared to both toxic and HCA solution-treated groups through exhibiting a low density of neutrophils. In addition, the ear chiefly restored its normal architecture after treatment. Furthermore, the epidermal layer exhibited higher thickness when compared with other groups.

at high surfactant concentrations. This in turn could decrease the viscosity of the colloidal system leading to enhancement of the escaping of drug molecules during the self-assembling process.[34,35]

*3.2.4. The Influence of Independent Variables on In Vitro Drug Release.* Drug release% was considered as one of the responses during the design as obtaining a controlled release system was one of our work aims. Drug release% of the 11 runs ranged between 58.9 and 85.9% (Table 2). Run 9 exhibited the lowest drug release%, while run 2 showed the highest Drug release% among all investigated formulations (Figure 2). The HCA release from all formulated batches exhibited a biphasic release behavior and an initial burst release (within first 4 h), followed by a sustained release over a longer period of time (the rest 8 h).

The initial rapid release of HCA might be attributed to the fast release of drug molecules adsorbed onto the surface of nanoparticles, whereas the terminal sustained release was attributed to the encapsulated drug, which slowly diffused through a similar matrix (both HCA and the lipomer matrix are hydrophobic).

According to statistical analysis of the results, both phospholipid concentration and surfactant concentration significantly ($p < 0.05$) influenced the release of drug from the HCA-loaded lipomers. Figure 1D shows the 3D response surface plot for drug release%, showing the effect of independent variables. The polynomial equation of drug release% is outlined below:

$$Y_4 = +74.03 - 9.32A + 3.8B - 0.6AB + 12.98A^2 - 15.22B^2 \quad (5)$$

As factor $A$ was negatively signed, it had an inverse relation with drug release%, i.e., the higher the phospholipid concentration, the slower the drug release. On the other hand, factor $B$ was positively signed, which indicated that it had a direct correlation with drug release%, i.e., the higher the surfactant concentration, the faster the drug release. As mentioned above, using a higher concentration of phospholipid led to an increase


https://doi.org/10.1021/acsomega.3c00638
ACS Omega 2023, 8, 18714−18725

in the thickness of the lipid layer,[32] which could hinder the release of the encapsulated drug. Enhancement of drug release upon increasing concentration of the surfactant might be attributed to the decrease in the particle size, which led to an improved dissolution rate. In addition, the presence of hydrophilic surfactants (such as Tween 80) alongside phospholipid at the surface of the system could modulate the drug release.[36]

The point prediction tool is the main purpose of the design to choose the optimum level of independent variables based on the obtained responses. According to Design software, we composed the optimum formulation outlined in Table 3, aiming to minimize the particle size, maximize the magnitude of the zeta potential, maximize the HCA encapsulation in lipomers, and control the HCA release. The optimized composition comprised phospholipid concentration (8.2 mg/mL) and Tween 80 concentration (0.675%). It showed a particle size of less than 210.7 nm, a zeta potential of −27.3 mV, an entrapment efficiency of 82.7%, and a drug release of 61.7%. It is obvious from the obtained findings that the predicted values of the dependent variables were in good agreement with the actual measurements, which reveals the reliability of the optimization process for the fabrication of HCA-loaded lipomers.[37]

**3.3. Morphology.** Figure 3A shows the morphology of the optimized formulation. The TEM image shows nanometric, discrete, and spherical particles. It is noticed that there was an inner bright color (suggested to be the PCL core), which was surrounded inside the phospholipid material indicating the homogenous distribution of the loaded drug.[38] The particle size presented in the TEM image was in good accordance with that measured by the Zetasizer (Figure 3B).

**3.4. Thermal Analysis.** Figure 4 displays the thermograms of HCA, PCL, phospholipid, and the optimized formulation. Pure HCA showed the main sharp endothermic peak at 225.35 °C (Figure 4A), which resembled that of raw HCA melting[39] and confirmed the presence of the drug in its highly stable lattice structure.[40] PCL (Figure 4B) presented a single endothermic peak at 69.83 °C. Phospholipid (Figure 4C) presented three somewhat broad peaks at 152.12, 164.89, and 238 °C, which correspond to the thermal pattern of amorphous substances.[41] The optimized formulation thermograms (Figure 4D) showed a clear presentation of one peak corresponding to that of PCL (with a slightly minimized intensity than the pure material) with complete loss of the HCA characteristic peak. Loss of the HCA main peak might be attributed to incorporation into the lipomer matrix, indicating either loss of its crystallinity to create an amorphous state or complete disorganization of the crystalline structure due to the lattice defects during formulation of the optimized formulation.[42,43]

**3.5. FTIR.** Figure 5 shows the spectra of HCA, phospholipid, PCL, and the optimized formulation. The FTIR spectrum of raw HCA showed the main peak at 3372 $cm^{-1}$, which indicated the presence of the −OH group, 2847 $cm^{-1}$ indicating aliphatic C−H stretching, 1703 and 1681 $cm^{-1}$ indicating the carbonyl group, and 1081 $cm^{-1}$ indicating C−O.[44] Phospholipid displayed distinct broad peaks at 3310 $cm^{-1}$ indicating −OH vibrational stretching,[45] 2917 and 2855 $cm^{-1}$ indicating C−H, 1733 $cm^{-1}$ indicating the carbonyl group of fatty acid ester, 1237 $cm^{-1}$ indicating −P=O stretching, and 964 $cm^{-1}$ indicating $-N^{+}(CH_2)_3$ stretching. Raw PCL showed a distinct broad peak at 3431 $cm^{-1}$ indicating the terminal −OH group, 2939 and 2861 $cm^{-1}$ indicating asymmetric and symmetrical $CH_2$ stretching, respectively,[46] 1710 $cm^{-1}$ indicating ester carbonyl group vibration,[47] and 1168 $cm^{-1}$ indicating C−H stretching of C−O stretching. In the case of the optimized formulation, the spectra showed most of the phospholipid and PCL characteristic peaks while most of the HCA peaks faded or disappeared in the spectra (dashed vertical yellow lines). This result refers to the presence of interactions between HCA and the lipomer matrix (phospholipid and PCL) and reveals that the HCA molecule was incorporated into the formulation.

**3.6. Stability Study.** The stability of the optimized formulation was carried out in terms of particle size, zeta potential, and EE% after 1 month at ambient and refrigerating temperatures (Table 4). The results showed that particle size, zeta potential, and EE% were slightly influenced at both room and refrigerating temperatures. However, no significant changes were detected in the evaluation parameters revealing good stability of the optimized formulation.

**3.7. Ex Vivo Skin Permeation.** Skin permeation study is one of important experiments during the design of topical formulations in order to investigate the capability of a loaded drug to diffuse through full-thickness skin and reach the underlying tissues. Figure 6 displays the cumulative percentage of HCA that permeated through the skin from the optimized formulation in comparison with the HCA solution. After 12 h, HCA permeated at a significant ($p < 0.05$) higher percentage (44.33 ± 1.5%) when compared to the HCA solution (22.23 ± 2.5%). Table 5 displays the findings of *Jss*, *Kp*, permeated amount per unit area (Q/A), and ER of HCA. As realized, the optimized formulation showed higher values of Q/A (38.88 ± 5.1 $\mu g/cm^2$), *Kapp* (11.84 ± 1.29 × $10^2$ cm/h), and *Jss* (0.987 ± 0.141 $\mu g/cm^2/h$) when compared to the HCA solution (19.50 ± 2.8 $\mu g/cm^2$, 7.95 ± 1.4 × $10^2$ cm/h and 0.663 ± 0.162 $\mu g/cm^2/h$ respectively), which totally accounted for 1.5-fold ER.

HCA is a neutral compound and suffers from low flux due to the comparatively poor aqueous solubility and inadequate solubilization capacity of the surface active agent.[39] Commonly, presenting the active molecules in nanosystems enhances skin permeability due to the presence of a large effective surface area of the nanosystem carrying the drug, which increases drug saturation solubility and creates a concentration gradient between the system and skin.[48]

Principally, lipomers can proficiently entrap lipophilic drugs in the polymeric core and possess good biocompatibility with biomembranes due to the presence of the phospholipid at the surface. The enhanced skin delivery in the case of the optimized formulation might be attributed to several factors. The small particle size of lipomers created an occlusive effect on the skin layer resulting in prolongation of the duration of action and increase in *Jss*.[49] In addition, polymer could sustain drug release. Furthermore, incorporation of phospholipid improved skin delivery via modulation of system flexibility (Phospholipon 90G is an unsaturated phospholipid), which prompts deep skin penetration.[50] Phospholipid improves the formulation compatibility with skin composition, and fusion with skin lipid could take place to augment permeability through the skin layers.[51] Tween 80 was also established to improve skin permeability by interaction with skin lipids then increases in its fluidity.[52] On the other hand, HCA solution was prepared by dissolving in aqueous solution of propylene glycol (50%; v/v). Propylene glycol might improve the skin permeability of HCA via production of saturated solution and thus maximizing the concentration gradient across the stratum corneum.[53] This might improve the permeability of the HCA solution to some extent.



https://doi.org/10.1021/acsomega.3c00638
ACS Omega 2023, 8, 18714−18725

Table 6 displays the kinetic parameters obtained by fitting the permeation data to various kinetic models. Based on the highest value of the correlation coefficient ($R^2$), the optimized formulation followed the Korsmeyer−Peppas model ($R^2$ = 0.987). It also showed a value of exponential ($n$) = 0.361 (less than 0.5), indicating that the permeation kinetics of HCA from the optimized formulation was controlled by Fickian diffusion.

**3.8. Histopathology.** In order to explore the effect of the optimized formulation on the histological structure, an insight of skin histopathology was done. Figure 7A displays the photomicrograph of rabbit dorsal skin sections of the control untreated group showing normal architecture and typical skin layers. Application of the optimized formulation (Figure 7B) exhibited higher thickness of the epidermal layer without neutrophil infiltration, confirming acceptable skin tolerability. Figure 8 shows the epidermal thickness of both the control and optimized formulation-treated groups. The thickness of the control group was significantly less (17.86 ± 3.29 $\mu$m) than that of the optimized formulation-treated group (32.86 ± 7.3 $\mu$m). This increment in the thickness of the epidermal layer reflects the occlusive effect of phospholipid-containing lipomers. This in turn could disturb the principal obstacle of the stratum corneum and enhance the cutaneous delivery, which was verified by ex vivo skin permeability studies.

**3.9. Pharmacodynamic Activity.** Evaluation of anti-inflammatory activity was assessed by the croton oil-induced rosacea model. Figure 9 shows photomicrographs of the rabbit ear sections of different groups. Figure 9A displays the histology of the untreated group, which shows normal architecture without any signs of inflammation. Figure 9B (toxic group) shows intense pathological changes verified by a high level of neutrophil infiltrations and approximately full detachment of the epidermis. Croton oil is a well-known irritant material, which motivates inflammatory reaction when topically painted to the skin.[54]

## 4. CONCLUSIONS

In this work, HCA-loaded lipomers composed of PCL as the polymeric core and phospholipid layer at the interface were successfully developed by a single-step nanoprecipitation method. The Box−Behnken design was effectively applied to optimize the influence of the phospholipid concentration and the concentration of the surfactant on different responses. The optimized formulation (composed of 8.2 mg/mL of phospholipid concentration and 0.675% Tween 80) showed a satisfying particle diameter, zeta potential, EE%, and controlled release pattern. It also showed a spherical morphology with suitable stability. Thermal analysis revealed that HCA lost its crystallinity when formulated in the optimized formulation. Ex vivo study showed a higher flux and permeability coefficient of HCA through the skin from the optimized formulation when compared with the HCA solution. Meanwhile, histological examination after topical application of the optimized formulation showed an increase in epidermal thickness with very minimal dermatotoxicity. In vivo, the optimized formulation exhibited excellent anti-inflammatory activity in the croton oil-induced rosacea model. These findings propose that the use of lipomer, as an excellent anti-inflammatory agent, could be a promising strategy to improve the topical effectiveness of HCA against different topical inflammatory diseases.

## ASSOCIATED CONTENT

### Supporting Information

The Supporting Information is available free of charge at https://pubs.acs.org/doi/10.1021/acsomega.3c00638.

Summary of regression analysis for the calculated responses (PDF)

## AUTHOR INFORMATION


### Corresponding Author

**Mohammed Elmowafy** − *Department of Pharmaceutics, College of Pharmacy, Jouf University, Sakaka 72341, Saudi Arabia;* orcid.org/0000-0002-2393-8195; Phone: +966541869569; Email: melmowafy@ju.edu.sa

### Authors

**Omar Awad Alsaidan** − *Department of Pharmaceutics, College of Pharmacy, Jouf University, Sakaka 72341, Saudi Arabia*

**Khaled Shalaby** − *Department of Pharmaceutics, College of Pharmacy, Jouf University, Sakaka 72341, Saudi Arabia*

**Sami I. Alzarea** − *Department of Pharmacology, College of Pharmacy, Jouf University, Sakaka 72341, Saudi Arabia*

**Diaa Massoud** − *Department of Biology, College of Science, Jouf University, Sakaka 72341, Saudi Arabia*

**Abdulsalam M. Kassem** − *Department of Pharmaceutics and Pharmaceutical Technology, Faculty of Pharmacy (Boys), Al-Azhar University, Nasr City, Cairo 11751, Egypt*

**Mohamed F. Ibrahim** − *Department of Pharmaceutics and Pharmaceutical Technology, Faculty of Pharmacy (Boys), Al-Azhar University, Nasr City, Cairo 11751, Egypt*

Complete contact information is available at: https://pubs.acs.org/10.1021/acsomega.3c00638



### Funding

This work was funded by the Deanship of Scientific Research at Jouf University under grant no. DSR-2021-01-03189.

### Notes

The authors declare no competing financial interest.

## ACKNOWLEDGMENTS

The authors acknowledge the financial support by the Deanship of Scientific Research at Jouf University.


## REFERENCES


(1) Hay, R. J.; et al. The global burden of skin disease in 2010: an analysis of the prevalence and impact of skin conditions. *J. Invest. Dermatol.* **2014**, *134*, 1527−1534.

(2) Lim, H. W.; et al. The burden of skin disease in the United States. *J. Am. Acad. Dermatol.* **2017**, *76*, 958−972.e2.

(3) Eroğlu, İ.; et al. Effective topical delivery systems for corticosteroids : dermatological and histological evaluations Effective topical delivery systems for corticosteroids : dermatological and histological evaluations. *Drug Delivery* **2016**, *7544*, 1502.

(4) Bieber, T.; et al. Clinical phenotypes and endophenotypes of atopic dermatitis: where are we, and where should we go? *J. Allergy Clin. Immunol.* **2017**, *139*, S58−S64.

(5) Weidinger, S.; Novak, N. Dermatitis atópica. *Lancet* **2016**, *387*, 1109−1122.

(6) Kondiah, P. P. D.; Rants'o, T. A.; Mdanda, S.; Mohlomi, L. M.; Choonara, Y. E. A Poly (Caprolactone)-Cellulose Nanocomposite Hydrogel for Transdermal Delivery of Hydrocortisone in Treating Psoriasis Vulgaris. *Polymer* **2022**, *14*, 2633.

(7) Devaraj, N. K.; Aneesa, A. R.; Abdul Hadi, A. M.; Shaira, N. Topical corticosteroids in clinical practice. *Med. J. Malaysia* **2019**, *74*, 187−189.
(8) Altamimi, M.; Haq, N.; Alshehri, S.; Qamar, W.; Shakeel, F. Enhanced skin permeation of hydrocortisone using nanoemulsion as potential vehicle. *ChemistrySelect* **2019**, *4*, 10084−10091.
(9) Elmowafy, M. Skin penetration/permeation success determinants of nanocarriers: Pursuit of a perfect formulation. *Colloids Surf., B* **2021**, *203*, No. 111748.
(10) Li, Q.; et al. A review of the structure, preparation, and application of NLCs, PNPs, and PLNs. *Nanomaterials* **2017**, *7*, 122.
(11) Wu, X. Y. Strategies for optimizing polymer-lipid hybrid nanoparticle-mediated drug delivery. *Expert Opin. Drug Deliv.* **2016**, *13*, 609−612.
(12) Valencia, P. M.; et al. Single-step assembly of homogenous lipid−polymeric and lipid− quantum dot nanoparticles enabled by microfluidic rapid mixing. *ACS Nano* **2010**, *4*, 1671−1679.
(13) Garg, N. K.; et al. Development and characterization of single step self-assembled lipid polymer hybrid nanoparticles for effective delivery of methotrexate. *RSC Adv.* **2015**, *5*, 62989−62999.
(14) Gajra, B.; Dalwadi, C.; Patel, R. Formulation and optimization of itraconazole polymeric lipid hybrid nanoparticles (Lipomer) using box behnken design. *DARU J. Pharm. Sci.* **2015**, *23*, 1−15.
(15) Siddique, M. I.; et al. Potential treatment of atopic dermatitis: Tolerability and safety of cream containing nanoparticles loaded with hydrocortisone and hydroxytyrosol in human subjects. *Drug Deliv. Transl. Res.* **2019**, *9*, 469−481.
(16) Chen, Y. Packaging selection for solid oral dosage forms. in *Developing Solid Oral Dosage Forms 637−651* (Elsevier, 2017).
(17) Elmowafy, M.; et al. Impact of nanostructured lipid carriers on dapsone delivery to the skin: in vitro and in vivo studies. *Int. J. Pharm.* **2019**, *572*, No. 118781.
(18) Tawfik, M. A.; Tadros, M. I.; Mohamed, M. I. Lipomers (lipid-polymer hybrid particles) of vardenafil hydrochloride: a promising dual platform for modifying the drug release rate and enhancing its oral bioavailability. *Aaps PharmSciTech* **2018**, *19*, 3650−3660.
(19) Benival, D. M.; Devarajan, P. V. Lipomer of doxorubicin hydrochloride for enhanced oral bioavailability. *Int. J. Pharm.* **2012**, *423*, 554−561.
(20) Dong, W.; et al. Chitosan based polymer-lipid hybrid nanoparticles for oral delivery of enoxaparin. *Int. J. Pharm.* **2018**, *547*, 499−505.
(21) Desai, P. R.; et al. Topical delivery of anti-TNF$\alpha$ siRNA and capsaicin via novel lipid-polymer hybrid nanoparticles efficiently inhibits skin inflammation in vivo. *J. Controlled Release* **2013**, *170*, 51−63.
(22) Ma, P.; et al. Local anesthetic effects of bupivacaine loaded lipid-polymer hybrid nanoparticles: in vitro and in vivo evaluation. *Biomed. Pharmacother.* **2017**, *89*, 689−695.
(23) Kashif, P. M.; et al. Development of Eudragit RS 100 microparticles loaded with ropinirole: optimization and in vitro evaluation studies. *AAPS pharmscitech* **2017**, *18*, 1810−1822.
(24) Ravi, P. R.; Vats, R.; Dalal, V.; Gadekar, N.; N, A. Design, optimization and evaluation of poly-$\varepsilon$-caprolactone (PCL) based polymeric nanoparticles for oral delivery of lopinavir. *Drug Dev. Ind. Pharm.* **2015**, *41*, 131−140.
(25) Gajra, B.; Patel, R. R.; Dalwadi, C. Formulation, optimization and characterization of cationic polymeric nanoparticles of mast cell stabilizing agent using the Box−Behnken experimental design. *Drug Dev. Ind. Pharm.* **2016**, *42*, 747−757.
(26) Patel, R. R.; Khan, G.; Chaurasia, S.; Kumar, N.; Mishra, B. Rationally developed core−shell polymeric-lipid hybrid nanoparticles as a delivery vehicle for cromolyn sodium: implications of lipid envelop on in vitro and in vivo behaviour of nanoparticles upon oral administration. *RSC Adv.* **2015**, *5*, 76491−76506.
(27) Sahoo, S. K.; Panyam, J.; Prabha, S.; Labhasetwar, V. Residual polyvinyl alcohol associated with poly (D, L-lactide-co-glycolide) nanoparticles affects their physical properties and cellular uptake. *J. Controlled Release* **2002**, *82*, 105−114.
(28) Liu, Y.; Pan, J.; Feng, S.-S. Nanoparticles of lipid monolayer shell and biodegradable polymer core for controlled release of paclitaxel: effects of surfactants on particles size, characteristics and in vitro performance. *Int. J. Pharm.* **2010**, *395*, 243−250.
(29) El Badawy, A. M.; Luxton, T. P.; Silva, R. G.; Scheckel, K. G.; Suidan, M. T.; Tolaymat, T. M. Impact of environmental conditions (pH, ionic strength, and electrolyte type) on the surface charge and aggregation of silver nanoparticles suspensions. *Environ. Sci. Technol.* **2010**, *44*, 1260−1266.
(30) Demir, B.; et al. Gold nanoparticle loaded phytosomal systems: synthesis, characterization and in vitro investigations. *RSC Adv.* **2014**, *4*, 34687−34695.
(31) Cheow, W. S.; Hadinoto, K. Factors affecting drug encapsulation and stability of lipid−polymer hybrid nanoparticles. *Colloids Surf., B* **2011**, *85*, 214−220.
(32) Dudhipala, N.; Janga, K. Y. Lipid nanoparticles of zaleplon for improved oral delivery by Box−Behnken design: optimization, in vitro and in vivo evaluation. *Drug Dev. Ind. Pharm.* **2017**, *43*, 1205−1214.
(33) Jain, D.; Athawale, R.; Bajaj, A.; Shrikhande, S.; Goel, P. N.; Gude, R. P. Studies on stabilization mechanism and stealth effect of poloxamer 188 onto PLGA nanoparticles. *Colloids Surf., B* **2013**, *109*, 59−67.
(34) Ferreira, M.; Chaves, L. L.; Lima, S. A. C.; Reis, S. Optimization of nanostructured lipid carriers loaded with methotrexate: a tool for inflammatory and cancer therapy. *Int. J. Pharm.* **2015**, *492*, 65−72.
(35) Maleki Dizaj, S.; Lotfipour, F.; Barzegar-Jalali, M.; Zarrintan, M.-H.; Adibkia, K. Application of Box−Behnken design to prepare gentamicin-loaded calcium carbonate nanoparticles. *Artif. Cells, Nanomedicine, Biotechnol* **2016**, *44*, 1475−1481.
(36) Hallan, S. S.; Kaur, P.; Kaur, V.; Mishra, N.; Vaidya, B. Lipid polymer hybrid as emerging tool in nanocarriers for oral drug delivery. *Artif. Cells, Nanomedicine, Biotechnol.* **2016**, *44*, 334−349.
(37) Venugopal, V.; et al. Optimization and in-vivo evaluation of isradipine nanoparticles using Box-Behnken design surface response methodology. *OpenNano* **2016**, *1*, 1−15.
(38) Tahir, N.; et al. Development and optimization of methotrexate-loaded lipid-polymer hybrid nanoparticles for controlled drug delivery applications. *Int. J. Pharm.* **2017**, *533*, 156−168.
(39) Chang, S.-L.; Banga, A. K. Transdermal iontophoretic delivery of hydrocortisone from cyclodextrin solutions. *J. Pharm. Pharmacol.* **2011**, *50*, 635−640.
(40) Grcic, J. F.; et al. Chitosan microspheres with hydrocortisone and hydrocortisone-hydroxypropyl-b-cyclodextrin inclusion complex. *Eur. J. Pharm. Sci.* **2000**, *9*, 373−379.
(41) Salama, A.; Badran, M.; Elmowafy, M.; Soliman, G. M. Spironolactone-loaded leciplexes as potential topical delivery systems for female acne: In vitro appraisal and ex vivo skin permeability studies. *Pharmaceutics* **2020**, *12*, 25.
(42) Mandal, B.; Mittal, N. K.; Balabathula, P.; Thoma, L. A.; Wood, G. C. Development and in vitro evaluation of core−shell type lipid−polymer hybrid nanoparticles for the delivery of erlotinib in non-small cell lung cancer. *Eur. J. Pharm. Sci.* **2016**, *81*, 162−171.
(43) de Mello, V. A.; Ricci-Júnior, E. Encapsulation of naproxen in nanostructured system: structural characterization and in vitro release studies. *Quim. Nova* **2011**, *34*, 933−939.
(44) Dehkharghani, R. A.; Hosseinzadeh, M.; Nezafatdoost, F.; Jahangiri, J. Application of methodological analysis for hydrocortisone nanocapsulation in biodegradable polyester and MTT assay. *Polym. Sci. Ser. A* **2018**, *60*, 770−776.
(45) Satapathy, D.; et al. Sunflower-oil-based lecithin organogels as matrices for controlled drug delivery. *J. Appl. Polym. Sci.* **2013**, *129*, 585−594.
(46) Govender, T.; et al. A novel melt-dispersion technique for simplistic preparation of chlorpromazine-loaded polycaprolactone nanocapsules. *Polymer* **2015**, *7*, 1145.
(47) Kumar, A.; Sawant, K. Encapsulation of exemestane in polycaprolactone nanoparticles: optimization, characterization, and release kinetics. *Cancer Nanotechnol.* **2013**, *4*, 57−71.


https://doi.org/10.1021/acsomega.3c00638
*ACS Omega* 2023, 8, 18714−18725

(48) Oktay, A. N.; Karakucuk, A.; Ilbasmis-Tamer, S.; Celebi, N. Dermal flurbiprofen nanosuspensions: Optimization with design of experiment approach and in vitro evaluation. *Eur. J. Pharm. Sci.* **2018**, *122*, 254−263.
(49) Wang, J. et al. An alternative choice of lidocaine-loaded liposomes : lidocaine-loaded lipid − polymer hybrid nanoparticles for local anesthetic therapy An alternative choice of lidocaine-loaded liposomes : lidocaine-loaded lipid − polymer hybrid nanoparticles for local anesthetic therapy. 2016, *7544*, 1254, DOI: 10.3109/10717544.2016.1141259.
(50) Abdel-rashid, R. S.; Helal, D. A.; Alaa-eldin, A. A. Polymeric versus lipid nanocapsules for miconazole nitrate enhanced topical delivery : in vitro and ex vivo evaluation. *Drug Delivery* **2022**, *29*, 294−304.
(51) Laouini, A.; Charcosset, C.; Fessi, H.; Holdich, R. G.; Vladisavljević, G. T. Preparation of liposomes: A novel application of microengineered membranes-From laboratory scale to large scale. *Colloids Surf., B* **2013**, *112*, 272−278.
(52) Cappel, M. J.; Kreuter, J. Effect of nonionic surfactants on transdermal drug delivery: I Polysorbates. *Int. J. Pharm.* **1991**, *69*, 143−153.
(53) Aulton, M. E.; Taylor, K. M. G. *Aulton's Pharmaceutics E-Book: The Design and Manufacture of Medicines;* (Elsevier Health Sciences, 2017).
(54) Pawlaczyk, I.; Lewik-Tsirigotis, M.; Capek, P.; Matulová, M.; Sasinková, V.; Dąbrowski, P.; Witkiewicz, W.; Gancarz, R. Effects of extraction condition on structural features and anticoagulant activity of F. vesca L. conjugates. *Carbohydr. Polym.* **2013**, *92*, 741−750.
(55) Griffiths, C. E. M.; Barker, J. N. W. N. Pathogenesis and clinical features of psoriasis. *Lancet* **2007**, *370*, 263−271.
(56) Ahluwalia, A. Topical glucocorticoids and the skin-mechanisms of action: an update. *Mediators Inflamm.* **1998**, *7*, 183−193.



https://doi.org/10.1021/acsomega.3c00638
*ACS Omega* 2023, 8, 18714−18725